

23

Summary

24 Climate change is affecting species' physiology, pushing environmental tolerance limits
25 and shifting distribution ranges. In addition to temperature and ocean acidification,
26 increasing levels of hyposaline stress due to extreme precipitation events and freshwater
27 runoff may be driving some of the reported recent range shifts in marine organisms.
28 Using 2D gel electrophoresis and tandem mass spectrometry, we characterized the
29 proteomic responses of the cold-adapted blue mussel species *Mytilus trossulus*, a native
30 to the Pacific coast of North America, and the warm-adapted *M. galloprovincialis*, a
31 Mediterranean invader that has replaced the native from the southern part of its range, but
32 may be limited from expanding north due to hyposaline stress. After exposing
33 laboratory-acclimated mussels for 4 h to two different experimental treatments of
34 hyposaline conditions and one control treatment (24.5 and 29.8 and 35.0 psu,
35 respectively) followed by a 0 and 24 h recovery at ambient salinity (35 psu), we detected
36 changes in the abundance of molecular chaperones of the endoplasmic reticulum (ER),
37 indicating protein unfolding, during stress exposure. Other common responses included
38 changes in small GTPases of the Ras-superfamily during recovery, which suggest a role
39 for vesicle transport, and cytoskeletal adjustments associated with cell volume, as
40 indicated by cytoskeletal elements such as actin, tubulin, intermediate filaments and
41 several actin-binding regulatory proteins. Changes of proteins involved in energy
42 metabolism and scavenging of reactive oxygen species (ROS) suggest a reduction in
43 overall energy metabolism during recovery. Principal component analyses of protein
44 abundances suggest that *M. trossulus* is able to respond to a greater hyposaline challenge
45 (24.5 psu) than *M. galloprovincialis* (29.8 psu), as shown by changing abundances of
46 proteins involved in protein chaperoning, vesicle transport, cytoskeletal adjustments by
47 actin-regulatory proteins, energy metabolism and oxidative stress. While proteins
48 involved in energy metabolism were lower in *M. trossulus* during recovery from
49 hyposaline stress, *M. galloprovincialis* showed higher abundances of those proteins at
50 29.8 psu, suggesting an energetic constraint in the invader but not the native congener.
51 Both species showed lower levels of oxidative stress proteins during recovery. In
52 addition, oxidative stress proteins associated with protein synthesis and folding in the ER,
53 showed lower levels during recovery in *M. galloprovincialis*, in parallel with ER

54 chaperones, indicating a reduction in protein synthesis. These differences may enable the
55 native *M. trossulus* to cope with greater hyposaline stress in the northern part of its range.
56 Furthermore, these differences may help *M. trossulus* to outcompete *M. galloprovincialis*
57 in the southern part of *M. trossulus*' current range, thereby preventing *M.*
58 *galloprovincialis* from expanding further north.

59

60 Key words: biogeography, climate change, *Mytilus galloprovincialis*, *Mytilus trossulus*,
61 osmotic stress, proteomics, salinity stress, systems biology

62

63

Introduction

64 Biogeographic distribution ranges of marine organisms are shifting due to climate
65 change, specifically rising atmospheric and oceanic temperatures, increasing acidity of
66 the ocean and more frequent and extreme precipitation events leading to greater
67 hyposaline stress in estuaries and coastal waters (Harley et al., 2006; IPCC, 2007; Min et
68 al., 2011; Pall et al., 2011). In order to assess which environmental stressor, either in
69 isolation or combination, will affect the physiology of marine organisms the most and
70 thus be the driving force for range shifts, we have to assess the physiological impacts of
71 thermal, pH as well as hyposalinity stressors. The realization that extreme precipitation
72 events may be a potential driving force for range shifts gives this research topic renewed
73 urgency to improve our predictions of the ecological impacts of climate change.

74 It is now evident that rising temperatures affect rates of physiological processes
75 and the integrity of the cell's macromolecular structure and thereby contribute to shifting
76 range limits (Hochachka and Somero, 2002; Pörtner, 2010; Tomanek, 2008; Tomanek
77 2010). Although more extreme precipitation events due to higher atmospheric humidity
78 levels associated with climate change have been documented (Groisman et al., 2005; Min
79 et al., 2011), biologists are only now starting to evaluate potential impacts of these
80 events, e.g. greater levels of hyposaline stress, on species distribution ranges (Levinton et
81 al., 2011). Extreme precipitation events will occur in a warmer world even if total
82 precipitation levels will not increase (Karl and Trenberth, 2003). Analyses of regional
83 past trends and projected future scenarios of precipitation and stream flow under different
84 climate scenarios and their potential biological impacts are available for Chesapeake Bay.

85 These suggest that winter-flow will increase but summer-flow will decrease, with an
86 overall increase of acute hyposaline stress conditions (Najjar et al., 2010). An analysis of
87 precipitation trends for the USA predicts an increase in extreme precipitation events for
88 some coastal regions in California (Groisman et al., 2005), but does not state whether that
89 will lead to heavier river flow rates.

90 In order to assess the effect of extreme precipitation events and their potential
91 impacts on shifting distribution ranges, we decided to investigate the physiological
92 responses to hyposaline stress of a pair of blue mussel species whose recent
93 biogeographic changes have been documented and linked to changes in both temperature
94 and salinity. One of the two blue mussel species is *Mytilus galloprovincialis*, which
95 invaded southern California during the middle of the last century and has replaced the
96 native *M. trossulus* from the southern part of its distribution range, from Baja California
97 to central California (Braby and Somero, 2006a; Geller, 1999; McDonald and Koehn,
98 1988; Rawson et al., 1999). Although the range limits of these congeners are still in flux
99 due to shorter climatic variations, e.g. Pacific Decadal Oscillation, the main hybrid zone
100 ranges roughly from Monterey Bay to San Francisco Bay, with small numbers of *M.*
101 *galloprovincialis* hybrids found further north to Humboldt Bay (Braby and Somero,
102 2006a; Hilbish et al., 2010). Field surveys indicate that the distribution within the hybrid
103 zone is determined by both temperature and salinity (Braby and Somero, 2006a;
104 Schneider and Helmuth, 2007). Salinity seems to play a critical role because *M. trossulus*
105 occurs at sites with higher freshwater input that are warm enough to normally favor
106 occurrence of the more warm-adapted *M. galloprovincialis* (Braby and Somero, 2006a).
107 Based on their natural distribution, the Eastern Pacific *M. trossulus* seem to prefer colder
108 temperatures and tolerate lower salinity levels, whereas the Mediterranean *M.*
109 *galloprovincialis* is a warm-water species that prefers high salinity levels (Seed, 1992).
110 Measurements of growth, heart rates and survival generally confirm these interspecific
111 differences (Braby and Somero, 2006b; Schneider, 2008). One hypothesis for the
112 underlying mechanistic differences is that *M. trossulus* may achieve tolerance to lower
113 salinities by closing their shells, as indicated by a drop in heart rate (Braby and Somero,
114 2006b).

115 In this study, we have chosen to focus on the proteome to characterize the

116 molecular mechanisms that set environmental tolerance limits, since changes in protein
117 abundance represent modifications of the molecular phenotype of the cell and therefore
118 functional changes (Feder and Walser, 2005). Mass spectrometry-enabled proteomic
119 analyses were first made possible with the completion of genome sequencing projects for
120 model organisms (Aebersold and Mann, 2003; Mann et al., 2001). Through advances in
121 mass spectrometry and the generation of expressed sequence tag (EST) libraries,
122 proteomic studies on non-model organisms have constantly improved, leading to the
123 generation of a number of new hypotheses about the stress responses of organisms to
124 environmental change (Tomanek, 2011; Tomanek, 2012).

125 By comparing proteomic responses to acute and chronic temperature stress in two
126 closely related species of *Mytilus* that vary in distribution and invasiveness, we have
127 generated several new hypotheses about how differently adapted congeners vary in their
128 cellular responses to thermal stress and which cellular processes are involved in setting
129 tolerance limits (Fields et al., 2012; Tomanek and Zuzow, 2010); simultaneously, our
130 collaborators focused on the transcriptomic responses of these congeners to acute heat
131 and hyposaline stress (Lockwood et al., 2010; Lockwood and Somero, 2011). Here we
132 exposed both blue mussel congeners to short exposures (4 h) of hyposaline stress (24.5
133 and 29.8 psu and a control of 35 psu) followed by a 0 and 24 h recovery at 35 psu, to
134 mimic conditions typical for bays and coastal areas experiencing heavy freshwater input
135 with a quick return to full salinity due to incoming tides and mixing with full-strength
136 seawater. Our results in the current study indicate that the native *M. trossulus* is able to
137 respond to a greater range of salinity variations than the invasive Mediterranean *M.*
138 *galloprovincialis*. This increased plasticity with respect to salinity tolerance may better
139 equip the native *M. trossulus* to compete with the invader in regions with warmer water
140 and more frequent hyposaline stress despite the invaders increased heat tolerance. Our
141 proteomic analysis implicates protein homeostasis, vesicle transport and cytoskeletal
142 rearrangements as well as modifications in energy metabolism and oxidative stress
143 response as cellular processes setting interspecific differences in salinity tolerance.

144

145

Materials and Methods

146

Animal collection, maintenance and experimental design

147 *Mytilus trossulus* (Gould 1850) and *M. galloprovincialis* (Lamarck 1819) were collected
148 subtidally from Newport, Oregon, USA (44°38'25" N, 124°03'10" W) and Santa Barbara,
149 California, USA (34°24'15" N, 119°41'30" W), respectively. In a separate study PCR
150 was used to confirm that each site was occupied by only a single species (i.e., there were
151 no hybrids present) (Lockwood et al., 2010). The experimental conditions were chosen
152 to simulate temporary hyposaline stress conditions as they occur in estuaries and bays
153 during heavy winter rains in California near the hybrid zone. However, these conditions
154 are often quickly reversed due to incoming tides and dilution of freshwater.

155 Animals were kept for four weeks under constant immersion at 13°C in re-
156 circulating seawater (SW) tanks with a salinity of 35 psu and fed a phytoplankton diet
157 (Phytofeast, Reed Mariculture Inc., Campbell, CA, USA) every day. We employed two
158 experimental treatments, 24.5 and 29.8 psu and one control treatment of 35.0 psu salinity.
159 All treatments were kept at 13°C for the duration of the experiments. Animals were
160 exposed for 4 h (or 0 h recovery), at which point we collected the first set of gill tissues
161 (N = 4-6 for all treatments). Another set was collected after a 24 h recovery period at
162 35.0 psu (N = 6 for each treatment). The actual osmolalities measured with an
163 osmometer (Advanced Instruments Inc., Norwood, MA, USA) were: 750, 858 and 979
164 mOsm/kg. The first time point was chosen because it coincides with the time of
165 collection of the samples used for the transcriptomic analysis (Lockwood and Somero,
166 2011), the second one because it allowed the organism to respond to the stress by
167 translating proteins in high enough abundances and assessed the proteomic response to a
168 hyperosmotic stress (relative to 24.5 and 29.8 psu) upon return to control conditions (35.0
169 psu). One possible behavioral response of *Mytilus* to hyposaline stress is shell closure to
170 avoid direct contact with the medium (Braby and Somero, 2006b), which would be
171 difficult to control. In order to avoid this confounding variable, we placed a small cork (5
172 mm diameter) between the shells to characterize the cellular response of gill tissue to the
173 three salinity treatments. Mussels were immediately dissected on chilled aluminum foil
174 and tissues were kept frozen at -80°C until processing.

175

176

Homogenization

177

Sample preparation followed the procedures outlined previously (Tomanek and

178 Zuzow, 2010). Briefly, gill tissue was lysed in homogenization buffer (7 mol l⁻¹ urea, 2
179 mol l⁻¹ thiourea, 1% ASB (amidofluorobetaine)-14, 40 mmol l⁻¹ Tris-base, 0.5%
180 immobilized pH 4-7 gradient (IPG) buffer (GE Healthcare, Piscataway, NJ, USA) and 40
181 mmol l⁻¹ dithiothreitol) at a ratio of 1:4. After centrifugation at 20°C for 30 min at
182 16,100 g, the proteins were precipitated by adding four volumes of ice-cold 10%
183 trichloroacetic acid in acetone and incubating the solution at -20°C overnight. The
184 precipitate was centrifuged at 4°C for 15 min at 18,000 g, the supernatant was discarded
185 and the protein pellet was washed with ice-cold acetone, and centrifuged again at 4°C.
186 After air-drying, the pellet was re-suspended in rehydration buffer (7 mol l⁻¹ urea, 2 mol l⁻¹
187 thiourea, 2% CHAPS (cholamidopropyl-dimethylammonio-propanesulfonic acid), 2%
188 NP (nonyl phenoxy polyethoxy ethanol)-40, 0.002% bromophenol blue, 0.5% IPG buffer
189 and 100 mmol l⁻¹ dithioerythritol). The protein concentration was determined with the
190 2D Quant kit (GE Healthcare), according to the manufacturer's instructions.

191

192 *Two-dimensional gel electrophoresis (2DGE)*

193 Prior to isoelectric focusing, IPG strips (pH 4-7, 11 cm; BioRad) were passively
194 rehydrated with 200 µL of 2.5 µg µl⁻¹ protein in rehydration buffer in wells for 13 h.
195 Isoelectric focusing was conducted using the following protocol : 250 V for 15 min,
196 gradient voltage increase to 8000 V for 1 h, 8000 V for 3 h 45 min, and reduced to 500 V
197 (Ettan IPGphor3, GE Heathcare, USA).

198 To prepare for 2nd dimension SDS-PAGE electrophoresis, strips were incubated in
199 equilibration buffer (375 mmol l⁻¹ Tris-base, 6 mol l⁻¹ urea, 30% glycerol, 2% SDS and
200 0.002% bromophenol blue) for two 15 min intervals, first with 65 mmol l⁻¹ dithiothreitol
201 and second with 135 mmol l⁻¹ iodoacetamide. IPG strips then were placed on top of
202 11.8% polyacrylamide gels, which were run (Criterion Dodeca; BioRad) at 200 V for 55
203 min at 10°C. Gels were subsequently stained with colloidal Coomassie Blue (G-250) and
204 destained with Milli-Q water for 48 h. The resulting gels were scanned with an Epson
205 1280 transparency scanner (Epson, Long Beach, CA, USA).

206

207 *Gel image analysis and statistical analysis of protein abundances*

208 Digitized images of 2D gels were analyzed using Delta2D (version 3.6; Decodon,

209 Greifswald, Germany) (Berth et al., 2007). Spot boundaries were detected on a fused
210 composite 2D gel image and transferred back to the original gel images. After
211 background subtraction, the relative amount of protein in each spot (i.e., spot volume)
212 was quantified by normalizing against total spot volume of all proteins in the image.

213 To determine which spots changed significantly in response to salinity (24.5, 29.8
214 and 35.0 psu) and recovery time (0 and 24 h), we used a two-way analysis of variance (P
215 < 0.02) with salinity and recovery time as the main effects and the effect of time on the
216 response to salinity as the interaction effect. We generated a null distribution for the two-
217 way ANOVA (1000 permutations) to account for unequal variance and non-normal
218 distributions of the response variables. In our result section we include all identified
219 proteins of certain functional categories and indicate if they showed significance for one
220 or both of the main effects and the interaction (Figs 4-6). The complete data set,
221 separated by main and interaction effects, is available in the supplemental material.
222 Since there is only limited overlap between the proteome maps of the two congeners, as
223 well as uncertainty whether overlapping proteins were orthologous or paralogous
224 homologs, a two-way ANOVA comparing species was not possible. Following the two-
225 way ANOVA, *post-hoc* testing to compare treatments was conducted using Tukey's
226 analysis ($P < 0.05$), using MiniTab (version 15; Minitab Inc., State College, PA, USA), to
227 support conclusions about differences in protein abundances (single protein graphs are
228 not shown).

229

230 *Mass spectrometry*

231 Proteins that changed abundance in response to temperature acclimation were
232 excised from gels and prepared for analysis by mass spectrometry (MS) following
233 previously published protocols (Fields et al., 2012; Tomanek and Zuzow, 2010).

234 We obtained peptide mass fingerprints (PMFs) using a matrix-assisted laser
235 desorption ionization tandem time-of-flight (MALDI-ToF-ToF) mass spectrometer
236 (Ultraflex II; Bruker Daltonics Inc., Billerica, MA, USA). We selected a minimum of six
237 and a maximum of 20 peptides for tandem MS in order to obtain information about their
238 b- and y-ions.

239 Analysis of peptide spectra followed previously published procedures (Fields et

240 al., 2012; Tomanek and Zuzow, 2010). We used flexAnalysis (version 3.0; Bruker
241 Daltonics Inc.) to detect peptide peaks (with a signal-to-noise ratio of 6 for MS and 1.5
242 for MS/MS). Porcine trypsin (Promega, Madison, WI) was used for internal mass
243 calibration.

244 To identify proteins we used Mascot (version 2.2; Matrix Science Inc., Boston,
245 MA, USA) and combined peptide mass fingerprints (PMFs) and tandem mass spectra in a
246 search against two databases. One database is an EST library that represents 12,961 and
247 1,688 different gene sequences for *Mytilus californianus* and *M. galloprovincialis*,
248 respectively (Lockwood et al. 2010). The other was NCBI, with 77410 total nucleotide
249 sequences with *Mytilus* as the taxonomic restriction, and 5266919 sequences under
250 Metazoa. Oxidation of methionine and carbamidomethylation of cysteine were our only
251 variable modifications. Our search allowed one missed cleavage during trypsin
252 digestion. For tandem MS we set the precursor-ion mass tolerance to 0.6 Da, the default
253 value in Mascot. The molecular weight search (MOWSE) score that indicated a
254 significant hit was dependent on the database: scores higher than 40 and 51 were
255 significant ($P < 0.05$) for a search in the *Mytilus* EST and NCBI database, respectively.
256 However, we only accepted positive identifications that included two matched peptides
257 regardless of the MOWSE score.

258

259 *Exploratory statistical analysis*

260 To associate proteins with similar changes in abundance across samples, we
261 employed hierarchical clustering with average linking (Delta2D), using a Pearson
262 correlation metric. To further assess the importance of specific proteins in differentiating
263 the proteomes of mussels exposed to different salinities we employed principal
264 component analysis (PCA; Delta2D) based on proteins whose abundances changed
265 significantly during and after exposure to hyposaline stress (two-way ANOVA; $P <$
266 0.02). Component loadings, which quantify the contribution of each protein in the
267 separation of samples along a given component, are reported in the supplemental material
268 as below or above ± 1.0 .

269

270

271

272

Results and Discussion

273

Salinity effects on protein abundances

274

Proteins from gill tissue of mussels exposed to three salinity levels (24.5, 29.8 and 35
275 psu) for 4 h and mussels that were given a chance to recover from these salinities at
276 control conditions (35.0 psu) for 24 h were separated by 2DGE and yielded 336 and 310
277 distinct protein spots in *M. trossulus* and *M. galloprovincialis*, respectively (Figs 1A and
278 1B). Of the total protein spots, 39% in *M. trossulus* and 29% in *M. galloprovincialis*
279 changed in response to hyposaline conditions.

280

In *M. trossulus*, principal component 1 (PC1) explains 27.4% of the variation of
281 protein abundance data and separates out the mussels exposed to 24.5 psu for 4 h
282 followed by exposure to 35.0 psu for 24 h during recovery (abbreviated 24.5 psu +24 h
283 from here on, Fig. 2A). Along the y-axis, PC2 explains 12.3% of the variation, and it
284 separates the control from the 29.8 psu treatment (Fig. 2A). These two PCs show that the
285 greatest variation in the data is found in the response of *M. trossulus* 24 h after an acute
286 exposure to 24.5 psu (PC1), followed by the variation between the control and 29.8 psu
287 treatments (PC2; Fig. 2A). These patterns suggest that the broadest proteomic
288 adjustments of gill tissue occur during recovery from 24.5 psu .

289

In *M. galloprovincialis* the contributions of PC1 and PC2 (26.6%, 14.0%,
290 respectively) to explaining the variation in protein abundance in response to hyposaline
291 treatment and recovery conditions are similar to *M. trossulus*. But in contrast to *M.*
292 *trossulus*, it is the 29.8 psu +24 h treatment that is separated the furthest from the other
293 treatments along PC1 (Fig. 2B). PC2 separates 29.8 psu 0 h from the remaining
294 treatments. Thus, PC1 and 2 indicate that the 29.8 psu hyposaline treatment causes the
295 largest variation in protein abundance in *M. galloprovincialis*, more so after +24 h than 0
296 h recovery.

297

Despite explaining similar levels of variation in protein abundance in both
298 species, the PCAs reveal differences in how the two species vary in their response to
299 hyposaline stress. In summary, *M. trossulus* responds strongest +24 h into the recovery
300 from a 24.5 psu exposure, whereas *M. galloprovincialis* responds strongest +24 h into the
301 recover from a 29.8 psu exposure while showing limited changes in protein abundance to

302 24.5 psu. The second component clusters three hyposaline conditions close to each other,
303 with the exception of 24.5 psu +24 h, and placed them in opposition to the control
304 treatments in *M. trossulus*, suggesting that these conditions require a similar proteomic
305 response and thus don't differ among each other enough to represent greatly differing
306 stress levels. In *M. galloprovincialis*, it is only the 29.8 psu 0 h exposure that is placed in
307 this position along PC2.

308

309 *Effects during recovery from hyposaline stress on protein abundances*

310 To assess the acute response as well as the recovery from hyposaline stress, we collected
311 samples at two time points, 0 h and +24 h into recovery (at 35.0 psu). This scenario
312 mimics the effect of a heavy-rain event diluting full-strength into more brackish SW, just
313 to return to full-strength SW after the cessation of the rain event, or more accurately, the
314 down-flow of a freshwater surface layer through an estuary or near coastal waters. Of the
315 336 proteins detected in *M. trossulus*, 27% (91 spots) changed during recovery, in *M.*
316 *galloprovincialis* 29% (or 89 of the 310 spots) changed.

317 In *M. trossulus*, PC1 explains 17.1% of the variation and separates the 24.5 psu
318 +24 h from the 0 h time point, with the 29.8 and 35.0 psu + 24 h treatments in-between
319 (Fig. 3A). PC2 explains 9.9% of the variation in *M. trossulus* and mainly separates the
320 29.8 and 35.0 psu +24 h treatments (negative on y-axis) from all other treatments.

321 In *M. galloprovincialis*, the first PC explained 28% of the variation in protein
322 abundance (Fig. 3B), about 11% more than in *M. trossulus*. Overall, PC1 separates all
323 +24 h from all 0 h treatments. The group separated the furthest along PC1 is 29.8 psu
324 +24 h. The other +24 h recovery treatments, 24.5 and 35.0 psu, are separated from 29.8
325 psu and overlap. PC2 in *M. galloprovincialis* explains 12.9% of the variation in protein
326 abundance and separates the 24.5 and 35.0 psu 0 h and 29.8 psu +24 h treatments
327 (positive range of PC2) from all others (Fig. 3B).

328 The PCAs show a clear separation with decreasing salinities during recovery in
329 *M. trossulus* along PC1 (Fig. 3A). There is little separation among the 0 h groups. This
330 suggests that most of the proteomic changes occur during recovery and are greater with
331 decreasing salinity.

332 *M. galloprovincialis* shows a similar pattern of separation along PC1, but with

333 29.8 instead of 24.5 psu +24 h being the treatment with the greatest separation and 24.5
334 and 35.0 psu +24 h overlapping (Fig. 3B).

335

336

Protein Homeostasis

337 Both species show species-specific changes in the abundance of chaperones that
338 are localized to the mitochondria, prohibitin (Liu et al., 2009), and the endoplasmic
339 reticulum (ER), e.g. 78kDa and 94kDa glucose regulated protein (GRP78 or BiP and
340 GRP94), protein disulfide isomerase (PDI) and translocon-associated protein β (part of
341 the Sec61 channel to translocate proteins during translation into the lumen of the ER)
342 (Araki and Nagata, 2012). GRP94 is a heat shock protein 90 homolog that facilitates
343 folding of secreted and membrane proteins and holds misfolded proteins until they can be
344 transported out of the ER for further degradation (Araki and Nagata, 2012; Eletto et al.,
345 2010). It also is a major calcium binding protein in the lumen of the ER and its up-
346 regulation is considered an indicator for ER stress, mainly because of its activation of
347 insulin-like growth factors, which facilitate recovery from ER stress while blocking
348 apoptosis (Eletto et al., 2010). GRP78 or BiP may precede GRP94 as a folding catalyst
349 (Melnick et al., 1994).

350 While *M. trossulus* showed the highest abundances of two GRP94 isoforms and
351 cystatin-B at 24.5 psu 0 h (Fig. 4A; cluster T_{CHA}), *M. galloprovincialis* increased
352 abundances of GRP94, two GRP78 isoforms, heat shock cognate (HSC) 70 and PDI at
353 29.8 psu 0 h (Fig. 4B; cluster G_{CHB}). These interspecific differences parallel our results
354 from the PCAs (Fig. 2) and suggest that *M. trossulus* is able to tolerate greater acute
355 hyposaline stress than *M. galloprovincialis* before disruption of proteostasis in the ER.

356 In addition, abundances of T-complex protein 1 (TCP-1), a tubulin- and actin-
357 folding chaperone decreased during hyposaline treatments (0 h) in *M. galloprovincialis*
358 only, suggesting that proper folding of cytoskeletal elements, such as building blocks for
359 cilia, was disrupted (Fig. 4B; Sternlicht et al., 1993). One small heat shock protein
360 (HSP), whose main function is to stabilize cytoskeletal elements (Haslbeck et al., 2005),
361 showed overall higher levels at all salinities at 0 h than after 24 h of recovery in *M.*
362 *galloprovincialis* (spot 41 was also identified as a small HSP but has a much higher than
363 expected molecular mass and thus may not be a small HSP). Together these data suggest

364 that proteostasis, especially in the ER, of the cytoskeleton and possibly cilia, is important
365 in setting species-specific limits to hyposaline stress in *Mytilus* gill tissue. Protein
366 folding in the ER is important for secreted proteins, especially as part of the mucus that is
367 transported across the ventral groove of the gill to capture food particles that will be
368 transported towards the mouth through ciliary movements.

369 The ER maintains an oxidizing environment that facilitates the formation of
370 disulfide bonds (Araki and Nagata, 2012; Csala et al., 2010). As a consequence, protein
371 folding in the ER is closely linked and sensitive to changes in the redox environment.
372 For example, abundance changes in GRP94 and PDI, a subfamily of the thioredoxin-like
373 proteins (Funato and Miki, 2007), represent key indicators for the disruption of
374 proteostasis in the ER (Eletto et al., 2010; Feige and Hendershot, 2011). Importantly,
375 reactive oxygen species (ROS) cannot only interrupt disulfide bonds but are actually
376 generated by the oxidation of sulfhydryl groups in the ER, specifically hydrogen
377 peroxide, and may make up as much as a quarter of all ROS produced in the cell (Araki
378 and Nagata, 2012; Csala et al., 2010; Malhotra and Kaufman, 2007). Furthermore, a
379 cluster of three proteins in *M. galloprovincialis* may play important roles in protein
380 folding or ROS scavenging in the ER: thioredoxin-like protein [a protein disulfide
381 reductase (Holmgren and Lu, 2010)], nucleoredoxin [a putative thioredoxin (Funato and
382 Miki, 2007)], and superoxide dismutase (Fig. 5B; cluster G_{EC}). Their abundances
383 decreased during recovery from 24.5 psu +24 h, possibly indicating a down-regulation of
384 protein folding activity and protein synthesis in the ER in response to hyposaline stress,
385 which would explain why the proteomic response at 24.5 psu in *M. galloprovincialis* was
386 closer to 35.0 psu than 29.8 psu (Fig. 2B).

387 Two proteins that are part of cluster G_{EC} (Fig. 5B), NADH dehydrogenase
388 (complex I of the electron transport chain [ETC]) and superoxide dismutase (SOD), are
389 shared between the congeners. While abundances of NADH dehydrogenase were overall
390 lower during recovery, they were comparatively higher at 29.8 psu +24 h in comparison
391 to 24.5 psu and the control +24 h treatments in both congeners (Figs 5A and B).
392 However, SOD showed decreasing abundances during recovery from 24.5 psu +24 h only
393 in *M. galloprovincialis*, in contrast to *M. trossulus*, which decreased SOD at 24.5 and
394 29.8 psu +24 h. Isoforms of NADP-dependent isocitrate dehydrogenase (NADP-ICDH)

395 are part of this cluster (Fig. 5A, cluster T_{EA}) and showed reduced abundances at 24.5 and
396 29.8 psu + 24 h in *M. trossulus*. We have hypothesized that all three proteins may play a
397 role in regulating oxidative stress, either through ROS production (NADH
398 dehydrogenase), ROS scavenging (SOD), or maintenance of high levels of reduced
399 glutathione for ROS scavenging in *Mytilus* in the mitochondria during acute heat stress
400 and acclimation to cold-temperature (NADP-ICDH)(Fields et al., 2012; Tomanek and
401 Zuzow, 2010). Of these three, at least NADP-ICDH has been shown to reside in the ER
402 (Margittai and Banhegyi, 2008) and could contribute to ROS scavenging in the ER. SOD
403 could scavenge the hydrogen peroxide normally produced during protein folding in the
404 ER.

405 The picture that emerges is one of protein unfolding in the ER during the acute
406 phase of hyposaline stress, as indicated by the up-regulation of the molecular chaperones
407 GRP78 and GRP94, with species-specific abundance patterns (e.g., 29.8 psu and 24.5 psu
408 in *M. galloprovincialis* and *M. trossulus*, respectively) and proteins (e.g. PDI in *M.*
409 *galloprovincialis*), followed by a reduction in protein synthesis and folding during
410 recovery, as indicated by reduced abundances of a subset of the same proteins [e.g.,
411 GRP78 and GRP94 at 29.8 psu and 24.5 psu in *M. galloprovincialis* and *M. trossulus*
412 [GRP94 spot 36 only], respectively). The proposed reduction in protein synthesis and
413 protein folding in the ER would cause a reduction in the production of ROS, specifically
414 H₂O₂, which may be indicated by the lower abundances of proteins involved in ER redox
415 regulation in *M. galloprovincialis* (thioredoxin-like and nucleoredoxin at 24.5 psu +24 h).
416 The lower abundances of additional oxidative stress proteins (SOD and NADP-ICDH),
417 possibly located in the ER or the nearby cytosol, during recovery also supports an
418 inference of lower levels of oxidative stress. Further support for the notion of reduced
419 protein synthesis may be coming from two proteins, HSC71 and translocon-associated
420 protein, from cluster T_{CHB} in *M. trossulus* (Fig. 4A), both of which showed increasingly
421 lower abundances with lower salinities during recovery (between 35 and 24.5 psu and
422 35/29.8 psu and 24.5 psu for HSC71 and translocon-associated protein, respectively) and
423 are indicators of chaperone activity of newly synthesized proteins that are processed
424 through the ER (Araki and Nagata, 2012). Although the comparison between the
425 congeners is suggestive, a more comprehensive characterization is necessary before we

426 can discern that differences in regulating the link between ER-localized protein
427 maturation and ROS production contribute to setting tolerance limits to hyposaline stress.

428 Finally, proteases break down irreversibly denatured proteins and thereby remove
429 them from a pool of possibly toxic aggregates that could interact with other functioning
430 proteins (Wong and Cuervo, 2012). In contrast to acute heat stress where we identified a
431 number of proteasome isoforms (Tomanek and Zuzow, 2010), in the current study we
432 identified only one proteasome α -type subunit in *M. trossulus* that showed higher
433 abundance at 24.5 psu +24 h (Fig. 4A). Cystatin-B is a protease inhibitor, especially of
434 cysteine proteases, which binds irreversibly to proteases and thereby protects cells from
435 their activity (Chapman et al., 1997). We identified three isoforms of cystatin-B, with
436 higher abundances during acute stress (spot 16), control conditions (spot 14) and during
437 recovery from extreme hyposaline stress (spot 15), with only minor shifts in molecular
438 mass and thus possibly suggesting a role for PTMs in regulating their activity.
439 Interestingly, cystatin-B together with fatty acid binding protein (FABP, see below; Fig.
440 6) have both been suggested to be urinary biomarkers for acute kidney injury (Vaidya et
441 al., 2008).

442

443 *Energy metabolism and oxidative stress*

444 Because the production of ROS is closely linked to the ETC and therefore to energy
445 metabolism, we cover both functional categories together (Murphy, 2009). Proteins
446 involved in energy metabolism and those indicating oxidative stress showed more
447 pronounced changes during recovery than during acute hyposaline stress in *M. trossulus*
448 (Fig. 5A). The hierarchical clustering showed two main patterns: one cluster with
449 abundances decreasing at either 24.5 or 29.8 psu or both during recovery (T_{EA}) and
450 another with increasing abundances mainly at 24.5 psu +24 h (T_{EB}). Proteins of cluster
451 T_{EA} (with the exception of ATP synthase [spot 6] and NADH dehydrogenase) showed
452 decreasing abundances in response to hyposaline stress during recovery. Proteins of this
453 cluster represent the pyruvate dehydrogenase (PDH) reaction (dihydrolipoyl
454 dehydrogenase [DLDH] is part of the PDH complex) as well as the Krebs cycle
455 (mitochondrial malate dehydrogenase [mMDH] and NADP-ICDH) and ATP production
456 (ATP synthase). With the exception of the latter enzyme, they were all hypothesized to

457 respond to increased ROS production by decreasing ROS-generating NADH-producing
458 pathways while increasing ROS-scavenging NADPH-producing pathways, in the case of
459 NADH-ICDH, during acute heat stress in *M. trossulus* (Tomanek and Zuzow, 2010). A
460 similar response may be seen here during recovery from hyposaline stress, with the
461 exception that abundances of NADP-ICDH did not increase. A possible reason for this
462 may be that we were not able to distinguish between the cytosolic (and ER) and the
463 mitochondrial isoforms of NADP-ICDH (Margittai and Banhegyi, 2008). However,
464 given that three typical oxidative stress proteins, DyP-type peroxidase (a
465 catalase)(Sugano, 2009), SOD and the mitochondrial isoform of aldehyde dehydrogenase
466 (ALDH)(Ellis, 2007) reduced abundances in parallel to the decreasing abundances of
467 NADH-producing enzymes suggests that the changes in proteins involved in energy
468 metabolism may be linked to reduced ROS production.

469 The complementary cluster (T_{EB}) mainly showed increasing abundances at 24.5
470 psu +24 h (Fig. 5A). The two ALDH isoforms are involved in the detoxification of
471 different species of aldehydes, which are produced in part through other ROS interacting
472 with the double bonds of polyunsaturated fatty acids and thus lipid peroxidation (Ellis,
473 2007). The electron transfer flavoprotein- α transfers electrons that are made available
474 through the β -oxidation of fatty acids via $FADH_2$ to the ETC (Salway, 2004). Finally,
475 propionyl CoA carboxylase plays a role in the metabolic pathways of valine, methionine
476 and threonine oxidation to succinyl CoA (Salway, 2004). These changes also indicate
477 increasing levels of one specific type of oxidative stress, possibly limited to a specific
478 group of macromolecules, e.g., lipids, as well as possible alternative strategies to regulate
479 energy metabolism to reduce ROS production.

480 *M. galloprovincialis* gill tissue showed three clusters: one with decreasing
481 abundances at 24.5 psu +24 h (Fig. 5B, G_{EC}), similar to the one discussed for *M.*
482 *trossulus* (Fig. 5A, T_{EA}), one with lower (G_{EA}) and one with higher abundances (G_{EB}) at
483 29.8 psu +24 h. Proteins involved in producing (PDH) and oxidizing NADH (NADH
484 dehydrogenase), as well as SOD as a scavenger of hydrogen peroxide, and
485 nucleoredoxin, a thioredoxin, and therefore a disulfide reductase (Funato and Miki,
486 2007), all showed lower abundances at 24.5 psu +24 h. In a direct comparison of the
487 same proteins (SOD and PDH or DLDH), *M. trossulus* showed lower abundances at 24.5

488 and 29.8 psu +24 h. These results are suggestive of an important role for a reduction in
489 energy metabolism, e.g. metabolic depression, in setting limits to hyposaline conditions,
490 possibly through the reduced production of ROS.

491 Clusters G_EA and G_EB are complementary and indicate that while ATP synthase
492 abundance is up, the abundances of oxidative stress proteins, such as DyP-type
493 peroxidase and peroxiredoxin 5, are down at 29.8 psu +24 h (Fig. 5B). The cytosolic
494 paralog of MDH (cMDH) showed two isoforms in both clusters, suggesting a possible
495 PTM, e.g. acetylation, regulating its activity (Zhao et al., 2010). This pattern suggests
496 that there may be a transitory increase in energy demand during recovery from 29.8 psu
497 in *M. galloprovincialis*.

498 In summary, during recovery from hyposaline stress metabolic pathways
499 involving NADH production and oxidation are down-regulated, to a greater extent in *M.*
500 *trossulus*, including exposure to both 24.5 and 29.8 psu +24 h, than in *M.*
501 *galloprovincialis*, which showed decreasing abundances only at 24.5 psu +24 h. These
502 changes are paralleled by decreasing abundances of oxidative stress proteins, with some
503 proteins likely localized to the ER where we hypothesize that they showed decreasing
504 abundances due to a decrease in protein synthesis and folding of proteins with disulfide
505 bridges, which in turn may lower the production of ROS. This link between reduced
506 protein synthesis and folding and lower levels of ROS production could be an
507 underappreciated reason for the translational arrest during stress (Holcik and Sonenberg,
508 2005). Two additional themes distinguished the proteomic response of the congeners: *M.*
509 *trossulus* showed changes in proteins indicating an up-regulation of metabolic pathways
510 (β -oxidation and metabolism of branched amino acids) at 24.5 psu +24 h that were not
511 seen in *M. galloprovincialis* and could indicate alternative metabolic pathways used by
512 *M. trossulus* during hyposaline stress. *M. galloprovincialis* showed increasing
513 abundances of ATP synthase but lower abundances of oxidative stress proteins at 29.8
514 psu +24 h, possibly indicating a transient increase in energy demand that *M. trossulus* did
515 not show.

516

517 *Cytoskeletal modifications and vesicular transport*

518 Proteins constituting the cytoskeleton or elements of cilia, actin binding and regulatory

519 proteins as well as small GTPases involved in vesicle formation and transport showed
520 three major clusters in *M. trussulus*: one in which five actins, one α -tubulin and gelsolin,
521 an actin severing protein (Silacci et al., 2004), showed higher abundances at mild (29.8
522 psu +24 h) but, in case of some proteins, lower abundances at extreme (24.5 psu +24 h)
523 hyposaline stress during recovery (Fig. 6A; cluster T_CC). A complementary cluster
524 showed higher abundances at extreme hyposaline stress and included three actins, a β -
525 tubulin, F-actin capping protein β , G-protein β , and Rab1-GDP dissociation inhibitor
526 (Rab1-GDI; cluster T_CA). Both clusters contain an isoform of the Na⁺/H⁺ exchange
527 regulatory factor (NHE-RF). A third cluster is characterized by lower abundances at one
528 or both hyposaline stress conditions during recovery (+24 h) and contains an actin, α -
529 tubulin, actophorin (a cofilin or actin depolymerization factor) and Ras-like GTPase Sar1
530 (cluster T_CB). Clusters T_CC and T_CB both contain an isoform of fatty acid binding
531 protein (FABP).

532 The distinct changes in clusters that mainly contain actin isoforms during
533 recovery with different levels of hyposaline stress (T_CA and T_CC) may be explained in
534 part by actin-binding and regulatory proteins that are also part of these clusters. For
535 example, at 24.5 psu +24 h abundances of actophorin and gelsolin are lower, while the F-
536 actin capping protein is up (Fig. 6A). Lower abundances of the former proteins indicate
537 that “tread milling” of actin or the growth of actin filaments, a process that can expand
538 the cell membrane and therefore cell volume, is inhibited upon return to control
539 conditions following extreme hyposaline stress (Le Clainche and Carlier, 2008). This
540 hypothesis is further supported by the simultaneously higher abundances of F-actin
541 capping protein, which would prevent actin filaments from growing.

542 We also identified two small GTPases, Ras-like GTPase Sar1, which recruits
543 membrane coat proteins that facilitate vesicle formation, and Rab1-GDI, a protein that
544 inhibits Rab1, which regulates vesicle transport from the ER to the Golgi apparatus (Di
545 Ciano-Oliveira et al., 2006; Marks et al., 2009). Thus, the simultaneously higher
546 abundance of Rab1-GDI and lower abundance of Ras-like GTPase Sar1 during recovery
547 from extreme hyposaline stress may be hypothesized to indicate a down-regulation of
548 vesicle formation and transport from the ER, possibly reversing the activation of these
549 processes during acute hyposaline stress (0 h).

550 Two isoforms of NHE-RF also changed in opposite clusters (T_{CA} and T_{CC}).
551 NHE-RF can be phosphorylated by protein kinase A and affects the signaling of G-
552 protein coupled receptors in addition to transporters (e.g., Na^+/H^+ exchanger), ion
553 exchangers and signaling proteins (Ardura and Friedman, 2011). Some NHE-RFs have a
554 C-terminal binding domain that connects them to the cytoskeleton, suggesting a role in
555 sensing cytoskeletal modifications and by extension cell volume (Thelin et al., 2005).
556 Given the difference in molecular mass between the isoforms (13 kDa), they may present
557 different orthologs rather than PTMs (Ardura and Friedman, 2011).

558 Finally, the role of the two FABP isoforms is unclear. Their abundance changes
559 are complementary, possibly because of PTMs (Fig. 6A). They may be involved in the
560 synthesis of lipids, including phospholipids, in the ER to modify membranes that may be
561 transported to the outer cell membrane (Storch and Thumser, 2000).

562 To understand the changes associated with the cytoskeleton and vesicle transport,
563 it is important to recall that the PCAs for *M. galloprovincialis* (Figs 2 and 3) showed
564 limited proteomic changes for the extreme hyposaline stress conditions. During acute
565 stress (0 h), proteins represented in cluster G_{CB} showed higher abundances at 29.8 psu
566 only (Fig. 6B). The majority of those are five and one isoforms of α - and β -tubulin,
567 respectively, three actins and Rab1-GDI, which would indicate that vesicle formation and
568 transport are inhibited during the early response to mild hyposaline stress. At least
569 during 0 h, cluster G_{CD} included proteins with lower abundances at 29.8 psu, such as
570 radial spoke head 9 (RSH9), a cilia protein, Rho-GDI, an inhibitor of the small GTPase
571 Rho, a β -tubulin, profilin, which is an actin-binding protein that increases the rate and
572 affects the direction of actin tread milling as well as prevents G-actin aggregation,
573 depending on its PTMs (Le Clainche and Carlier, 2008), and two isoforms of myosin
574 light chain 1, which may be connecting actin and myosin near the periphery of the cell
575 (Estevez-Calvar et al., 2011). The cluster is in some way complementary to G_{CB} , at least
576 during the acute phase of the stress.

577 During recovery (+24 h), proteins of cluster G_{CA} showed higher abundances at
578 mild hyposaline stress (Fig. 6B). They include α - and β -tubulins, intermediate filament
579 and two isoforms of RSH. This cluster is similar to G_{CB} (higher abundances at 0 h) in
580 that it contains several tubulin isoforms. Cluster G_{CC} showed the opposite patterns

581 during recovery (+24 h) and contains three actins, β -tubulin and F-actin capping protein.
582 Although species-specific patterns of protein abundance exist, namely the greater
583 number of tubulin isoforms changing abundance in *M. galloprovincialis* but not *M.*
584 *trossulus* (Figs 6A and 6B), and specific proteins that were only identified for one of the
585 congeners, e.g. Ras-like GTPase Sar1 and FABP in *M. trossulus*, these differences and
586 the proteins the congeners have in common point to a related cellular response to
587 hyposaline stress. This response includes vesicle formation and transport in response to
588 osmotic cell swelling (van der Wijk et al., 2003), represented in part by the small
589 GTPases known to affect this process (Di Ciano-Oliveira et al., 2006; Marks et al., 2009).
590 In addition, vesicle transport, with a close connection to modifications to cilia
591 architecture, occurs with the help of tubulin, and depends on radial spokes (Silverman
592 and Leroux, 2009). The other cell-volume associated set of proteins includes the actin-
593 based cytoskeleton, specifically actin “tread milling” (Le Clainche and Carrier, 2008),
594 which seems to be regulated during recovery (Figs 6A and 6B). The species-specific
595 patterns point to a role for tubulin, and possibly its PTMs, specifically acetylation, as an
596 important process in affecting vesicle transport and cytoskeletal rearrangements (Perdiz
597 et al., 2011), and thereby reduced tolerance towards hyposaline conditions in *M.*
598 *galloprovincialis*. This hypothesis is further supported by the observation of decreasing
599 abundances of Rho-GDI, an inhibitor of the small GTPase Rho, which has been shown to
600 control this process (Destaing et al., 2005), in *M. galloprovincialis* during mild
601 hyposaline stress. Rho also affects several downstream protein kinases, which in turn
602 either indirectly through additional kinases or directly affect myosin light chains and
603 thereby cell volume, the cellular stress response, several actin-binding proteins as well as
604 the formation of actin stress fibers (Di Ciano-Oliveira et al., 2006; Marks et al., 2009).
605 These changes in addition to those directly linked to vesicle formation and transport
606 suggest that small GTPases-mediated processes contribute to setting species-specific
607 limits to hyposaline conditions.

608

609

Conclusion

610 The proteomic response of both *Mytilus* congeners to hyposaline stress showed common
611 themes: ER molecular chaperones indicate protein unfolding during the acute phase,

612 vesicle transport and cytoskeletal modifications suggest adjustments in cell volume,
613 especially during recovery, and proteins involved in energy metabolism and ROS
614 scavenging indicate that a reduction in energy demand may be accompanied by reduced
615 ROS production, also during recovery. However, the differences in protein abundances
616 suggest that *M. trossulus* can respond to a greater hyposaline challenge (24.5 psu) than
617 *M. galloprovincialis* (29.8 psu), specifically during recovery. It is possible that a
618 reduction of protein folding in the ER, during recovery, may be linked to decreased
619 oxidative stress in the ER, thereby lowering ROS production and, as a possible
620 consequence, protein denaturation (Dalle-Donne et al., 2003), more so in *M.*
621 *galloprovincialis* than in *M. trossulus*. Both vesicle transport and cytoskeletal
622 modifications play a role in the response to hyposaline stress. While *M. trossulus* showed
623 a number of actin-binding regulatory proteins changing abundances, *M. galloprovincialis*
624 showed a number of tubulin isoforms changing. While the former changes may be linked
625 to adjustments in cell volume, the latter changes may be linked to the transport of
626 membrane vesicles, possibly to first increase cell volume during acute hyposaline stress
627 and then to retrieve membranes during recovery. Changes in proteins involved in energy
628 metabolism indicate an overall reduction in energy metabolism upon return to control
629 conditions in both congeners, with an indication of a transient increase in energy
630 metabolism at mild hyposaline stress (29.8 psu) during recovery in *M. galloprovincialis*,
631 suggesting differences in time course and scope of adjustment in energy metabolism
632 between the congeners. In general, abundances in oxidative stress proteins parallel
633 changes of proteins involved in energy metabolism.

634 Abundance changes of ER-chaperones in response to osmotic stress have also
635 been observed in proteomic analyses of mouse embryonic stem cells and mouse kidney
636 cells (Dihazi et al., 2005; Mao et al., 2008). Proteins involved in small GTPase and
637 cytoskeletal pathways were enriched in osmoregulatory tissues of sharks (Lee et al.,
638 2006). Several of the proteins representing energy metabolism in *Mytilus* were also
639 found in the rectal glands of sharks in response to a feeding-associated salt load (Dowd et
640 al., 2008), but shark gill tissue showed a number of proteasome isoforms in response to
641 salinity change (Dowd et al., 2010), a response that was almost absent in *Mytilus*. Our
642 results indicate that these cellular processes play an important role in setting tolerance

643 limits towards hyposaline stress. Furthermore, the number of actin-binding regulatory
644 proteins and tubulin isoforms potentially associated with vesicle transport, provide novel
645 insights into the cellular processes contributing to salinity tolerance limits, especially in
646 gill tissue, which excretes proteins as part of the mucus needed to trap food. A
647 comparison of the proteomic responses of *Mytilus* gill tissue to acute heat stress and
648 temperature acclimation with the current data set shows some stressor specific cellular
649 processes, e.g. protein degradation during acute heat stress, as well as responses that are
650 common to all of the stressors, e.g. a trade-off between energy metabolism and oxidative
651 stress (Tomanek, 2012). Together these studies emphasize the importance of oxidative
652 stress and the comparisons between *Mytilus* congeners suggest that ROS-induced
653 physiological tolerance limits play an important role in setting biogeographic distribution
654 limits.

655 Finally, unlike our proteomic analysis, the transcriptomic analysis of gill tissue of
656 *Mytilus* specimens from the same experiment (but limited to the 35 and 29.8 psu +0 h
657 treatments) showed very few changes between the congeners (Lockwood and Somero,
658 2011). In addition, there is almost no overlap between the transcript and our protein
659 abundance changes, suggesting that interspecific differences at the level of the proteome
660 are crucial to setting tolerance limits to hyposaline stress. Some of the proteomic
661 changes observed here are likely based on PTMs, e.g. FABP in *M. trossulus* (Fig. 6A), a
662 conclusion that is supported by changes in protein kinase activities during hyposaline
663 stress in *Mytilus* (Evans and Somero, 2010).

664 Thus, the comparison of the proteomic responses of gill tissue of both congeners
665 to hyposaline stress conditions shows that, at the level of the molecular phenotype, the
666 warm-adapted *M. galloprovincialis* may be limited in its expansion north by an increase
667 in precipitation events and increased freshwater input near coastal waters. Moreover, it is
668 significant to note that this study illustrates possible molecular level mechanisms to
669 predict the results of closely related species competition in response to climate change.

670

671

LIST OF ABBREVIATIONS

672 ATP adenosine triphosphate
673 ALDH aldehyde dehydrogenase

674	ANOVA	analysis of variance
675	ASB-14	amidofolbetaine-14
676	BiP	binding immunoglobulin protein
677	CCT	chaperonin containing TCP-1
678	CHAPS	cholamidopropyl-dimethylammonio-propanesulfonic acid
679	DLDH	dihydrolipoyl dehydrogenase
680	ER	endoplasmic reticulum
681	EST	expressed sequence tag
682	ETC	electron transport chain
683	FABP	fatty-acid binding protein
684	F(G)-actin	filamentous (globular) –actin
685	FADH ₂	flavin adenine dinucleotide dihydrogen
686	GRP	glucose-regulated protein
687	G(D)TP	guanosine 5'-(di-)triphosphate
688	G _C A	<i>M. galloprovincialis</i> ; cytoskeleton-associated proteins; cluster A
689	G _{CH} A	<i>M. galloprovincialis</i> ; protein chaperoning/degradation; cluster A
690	G _E A	<i>M. galloprovincialis</i> ; energy metabolism; cluster A
691	HSP	heat shock protein
692	HSC	heat shock protein cognate
693	ICDH	isocitrate dehydrogenase
694	IPG	immobilized pH gradient
695	(c/m) MDH	(cytosolic/mitochondrial) malate dehydrogenase
696	MALDI-ToT-ToF	matrix-assisted laser desorption ionization tandem time-of-flight
697	MOWSE	molecular weight search
698	MS/MS	tandem mass spectrometry
699	NAD(H)	nicotinamide adenine dinucleotide (reduced form)
700	NADP(H)	nicotinamide adenine dinucleotide phosphate (reduced form)
701	NP-40	nonyl phenoxy polyethoxy ethanol 40
702	NHE-RF	Na ⁺ /H ⁺ exchange regulatory factor
703	PAGE	polyacrylamide gel electrophoresis
704	PC	principal component

705	PCA	principal component analysis
706	PDH	pyruvate dehydrogenase
707	PDI	protein disulfide isomerase
708	PMF	peptide mass fingerprint
709	PTM	post-translational modification
710	Rab-GDI	Rat Brain (small GTPase) - GDP dissociation inhibitor
711	Ras	Rat-sarcoma (small GTPase)
712	Rho	Ras-homology (small GTPase)
713	ROS	reactive oxygen species
714	RSH	radial spoke head
715	SAR	Secretion-associated Ras-like (small GTPase)
716	Sec61	ER protein transport protein
717	SDS	sodium dodecyl sulfate
718	SOD	superoxide dismutase
719	SW	seawater
720	TCP-1	T-complex protein 1
721	T _{CA}	<i>M. trossulus</i> ; cytoskeleton-associated proteins; cluster A
722	T _{CHA}	<i>M. trossulus</i> ; protein chaperoning/degradation; cluster A
723	T _{EA}	<i>M. trossulus</i> ; energy metabolism; cluster A
724	2DGE	two-dimensional gel electrophoresis

725

726 ***Acknowledgement***

727 We like to thank Daniel D. Magee, Jeremy K. LaBarge, and Brent L. Lockwood for their
728 assistance in conducting the original experiment. The experimental design was done in
729 collaboration with Drs Brent L. Lockwood and George N. Somero of Stanford University
730 (Lockwood and Somero, 2011). Drs Peter Field and Jennifer Oquendo, and Shelley
731 Blackwell provided helpful editorial suggestions. The proteomic analysis of this
732 collaboration was supported by National Science Foundation grant IOS-0717087 to L. T.

733

734

735

736 **References:**

- 737 **Aebersold, R. and Mann, M.** (2003). Mass spectrometry-based proteomics.
738 *Nature* **422**, 198-207.
- 739 **Araki, K. and Nagata, K.** (2012). Protein folding and quality control in the ER.
740 In *Protein Homeostasis*, eds. R. I. Morimoto D. J. Selkoe and J. W. Kelley, pp. 121-145.
741 New York: Cold Spring Harbor Press.
- 742 **Ardura, J. A. and Friedman, P. A.** (2011). Regulation of G protein-coupled
743 receptor function by Na⁺/H⁺ exchange regulatory factors. *Pharmacological Reviews* **63**,
744 882-900.
- 745 **Berth, M., Moser, F. M., Kolbe, M. and Bernhardt, J.** (2007). The state of the
746 art in the analysis of two-dimensional gel electrophoresis images. *Applied Microbiology*
747 *and Biotechnology* **76**, 1223-1243.
- 748 **Braby, C. E. and Somero, G. N.** (2006a). Ecological gradients and relative
749 abundance of native (*Mytilus trossulus*) and invasive (*M. galloprovincialis*) blue mussels
750 in the California hybrid zone. *Marine Biology* **148**, 1249-1262.
- 751 **Braby, C. E. and Somero, G. N.** (2006b). Following the heart: temperature and
752 salinity effects on heart rate in native and invasive species of the blue mussels (genus
753 *Mytilus*). *Journal of Experimental Biology* **209**, 2554-2566.
- 754 **Chapman, H. A., Riese, R. J. and Shi, G. P.** (1997). Emerging roles for cysteine
755 proteases in human biology. *Annual Review of Physiology* **59**, 63-88.
- 756 **Csala, M., Margittai, E. and Banhegyi, G.** (2010). Redox control of
757 endoplasmic reticulum function. *Antioxidant & Redox Signaling* **13**, 77-108.
- 758 **Dalle-Donne, I., Rossi, R., Giustarini, D., Milzani, A. and Colombo, R.** (2003).
759 Protein carbonyl groups as biomarkers of oxidative stress. *Clinica Chimica Acta* **329**, 23-
760 38.
- 761 **Destaing, O., Saltel, F., Gilquin, B., Chabadel, A., Khochbin, S., Ory, S. and**
762 **Jurdic, P.** (2005). A novel Rho-mDia2-HDAC6 pathway controls podosome patterning
763 through microtubule acetylation in osteoclasts. *Journal of Cell Science* **118**, 2901-2911.
- 764 **Di Ciano-Oliveira, C., Thirone, A. C., Szaszi, K. and Kapus, A.** (2006).
765 Osmotic stress and the cytoskeleton: the R(h)ole of Rho GTPases. *Acta Physiologicae*
766 (*Oxf*) **187**, 257-272.

767 **Dihazi, H., Asif, A. R., Agarwal, N. K., Doncheva, Y. and Muller, G. A.**
768 (2005). Proteomic analysis of cellular response to osmotic stress in thick ascending limb
769 of Henle's loop (TALH) cells. *Molecular & Cellular Proteomics* **4**, 1445-1458.

770 **Dowd, W. W., Harris, B. N., Cech, J. J., Jr. and Kultz, D.** (2010). Proteomic
771 and physiological responses of leopard sharks (*Triakis semifasciata*) to salinity change.
772 *Journal of Experimental Biology* **213**, 210-224.

773 **Dowd, W. W., Wood, C. M., Kajimura, M., Walsh, P. J. and Kültz, D.** (2008).
774 Natural feeding influences protein expression in the dogfish shark rectal gland: A
775 proteomic analysis. *Comparative Biochemistry and Physiology, Part D* **3**, 118-127.

776 **Eletto, D., Dersh, D. and Argon, Y.** (2010). GRP94 in ER quality control and
777 stress responses. *Seminars in Cell and Developmental Biology* **21**, 479-485.

778 **Ellis, E. M.** (2007). Reactive carbonyls and oxidative stress: potential for
779 therapeutic intervention. *Pharmacology and Therapeutics* **115**, 13-24.

780 **Estevez-Calvar, N., Romero, A., Figueras, A. and Novoa, B.** (2011).
781 Involvement of pore-forming molecules in immune defense and development of the
782 Mediterranean mussel (*Mytilus galloprovincialis*). *Developmental and Comparative*
783 *Immunology* **35**, 1017-1131.

784 **Evans, T. G. and Somero, G. N.** (2010). Phosphorylation events catalyzed by
785 major cell signaling proteins differ in response to thermal and osmotic stress among
786 native (*Mytilus californianus* and *Mytilus trossulus*) and invasive (*Mytilus*
787 *galloprovincialis*) species of mussels *Physiological and Biochemical Zoology* **83**, 984-
788 996.

789 **Feder, M. E. and Walser, J. C.** (2005). The biological limitations of
790 transcriptomics in elucidating stress and stress responses. *Journal of Evolutionary*
791 *Biology* **18**, 901-910.

792 **Feige, M. J. and Hendershot, L. M.** (2011). Disulfide bonds in ER protein
793 folding and homeostasis. *Current Opinion in Cell Biology* **23**, 167-175.

794 **Fields, P. A., Zuzow, M. J. and Tomanek, L.** (2012). Comparative proteomics
795 of blue mussel (*Mytilus*) congeners to temperature acclimation. *Journal of Experimental*
796 *Biology* **215**, 1106-1116.

797 **Funato, Y. and Miki, H.** (2007). Nucleoredoxin, a novel thioredoxin family

798 member involved in cell growth and differentiation. *Antioxidant & Redox Signaling* **9**,
799 1035-1057.

800 **Geller, J. B.** (1999). Decline of a native mussel masked by sibling species
801 invasion. *Conservation Biology* **13**, 661-664.

802 **Groisman, P. Y., Knight, R. W., Easterling, D. R., Karl, T. R., Hegerl, G. C.**
803 **and Razuvaev, V. N.** (2005). Trends in intense precipitation in the climate record.
804 *Journal of Climate* **18**, 1326-1350.

805 **Harley, C. D. G., Hughes, A. R., Hultgren, K., Miner, B. G., Sorte, C. J. B.,**
806 **Thornber, C. S., Rodrigues, L. F., Tomanek, L. and Williams, S. L.** (2006). The
807 impacts of climate change in coastal marine systems. *Ecology Letters* **9**, 228-241.

808 **Haslbeck, M., Franzmann, T., Weinfurtner, D. and Buchner, J.** (2005). Some
809 like it hot: the structure and function of small heat-shock proteins. *Nature Structural and*
810 *Molecular Biology* **12**, 842-846.

811 **Hilbish, T. J., Brannock, P. M., Jones, K. R., Smith, A. B., Bullock, B. N. and**
812 **Wethey, D. S.** (2010). Historical changes in the distributions of invasive and endemic
813 marine invertebrates are contrary to global warming predictions: the effects of decadal
814 climate oscillations. *Journal of Biogeography* **37**, 423-431.

815 **Hochachka, P. W. and Somero, G. N.** (2002). Biochemical adaptation:
816 Mechanism and process in physiological evolution. Oxford: Oxford University Press.

817 **Holcik, M. and Sonenberg, N.** (2005). Translational control in stress and
818 apoptosis. *Nature Review Molecular and Cellular Biology* **6**, 318-327.

819 **Holmgren, A. and Lu, J.** (2010). Thioredoxin and thioredoxin reductase: current
820 research with special reference to human disease. *Biochemical and Biophysical Research*
821 *Communications* **396**, 120-124.

822 **IPCC.** (2007). Climate Change 2007 - The Physical Science Basis. Cambridge:
823 Cambridge University Press.

824 **Karl, T. R. and Trenberth, K. E.** (2003). Modern global climate change.
825 *Science* **302**, 1719-1723.

826 **Le Clainche, C. and Carlier, M. F.** (2008). Regulation of actin assembly
827 associated with protrusion and adhesion in cell migration. *Physiological Reviews* **88**, 489-
828 513.

829 **Lee, J., Valkova, N., White, M. P. and Kültz, D.** (2006). Proteomic
830 identification of processes and pathways characteristic of osmoregulatory tissues in spiny
831 dogfish shark (*Squalus acanthias*). *Comparative Biochemistry and Physiology, Part D* **1**,
832 328-343.

833 **Levinton, J., Doall, M., Ralston, D., Starke, A. and Allam, B.** (2011). Climate
834 change, precipitation and impacts on an estuarine refuge from disease. *PLoS One* **6**,
835 e18849.

836 **Liu, X., Ren, Z., Zhan, R., Wang, X., Wang, X., Zhang, Z., Leng, X., Yang, Z.**
837 **and Qian, L.** (2009). Prohibitin protects against oxidative stress-induced cell injury in
838 cultured neonatal cardiomyocyte. *Cell Stress and Chaperones* **14**, 311-319.

839 **Lockwood, B. L., Sanders, J. G. and Somero, G. N.** (2010). Differences in
840 transcriptomic responses to heat-stress in native and invasive blue mussels (genus
841 *Mytilus*): molecular correlates of invasive success. *Journal of Experimental Biology* **213**,
842 3548-3558.

843 **Lockwood, B. L. and Somero, G. N.** (2011). Transcriptomic responses to
844 salinity stress in invasive and native blue mussels (genus *Mytilus*). *Molecular Ecology* **20**,
845 517-529.

846 **Malhotra, J. D. and Kaufman, R. J.** (2007). The endoplasmic reticulum and the
847 unfolded protein response. *Seminars in Cell and Developmental Biology* **18**, 716-731.

848 **Mann, M., Hendrickson, R. C. and Pandey, A.** (2001). Analysis of proteins and
849 proteomes by mass spectrometry. *Annual Review of Biochemistry* **70**, 437-473.

850 **Mao, L., Hartl, D., Nolden, T., Koppelstatter, A., Klose, J., Himmelbauer, H.**
851 **and Zabel, C.** (2008). Pronounced alterations of cellular metabolism and structure due to
852 hyper- or hypo-osmosis. *Journal of Proteome Research* **7**, 3968-3983.

853 **Margittai, E. and Banhegyi, G.** (2008). Isocitrate dehydrogenase: A NADPH-
854 generating enzyme in the lumen of the endoplasmic reticulum. *Archives of Biochemistry*
855 *and Biophysics* **471**, 184-190.

856 **Marks, F., Klingmüller, U. and Müller-Decker, K.** (2009). Cellular signal
857 processing: An introduction to the molecular mechanisms of signal transduction. New
858 York: Garland Science, Taylor and Francis Group

859 **McDonald, J. H. and Koehn, R. K.** (1988). The mussels *Mytilus*

860 *galloprovincialis* and *Mytilus trossulus* on the Pacific coast of North America. *Marine*
861 *Biology* **99**, 111-118.

862 **Melnick, J., Dul, J. L. and Argon, Y.** (1994). Sequential interaction of the
863 chaperones BiP and GRP94 with immunoglobulin chains in the endoplasmic reticulum.
864 *Nature* **370**, 373-375.

865 **Min, S. K., Zhang, X., Zwiers, F. W. and Hegerl, G. C.** (2011). Human
866 contribution to more-intense precipitation extremes. *Nature* **470**, 378-381.

867 **Murphy, M. P.** (2009). How mitochondria produce reactive oxygen species.
868 *Biochemical Journal* **417**, 1-13.

869 **Najjar, R. G., Pyke, C. R., Adams, M. B., Breitburg, D., Hershner, C., Kemp,**
870 **M., Howarth, R. W., Mulholland, M. R., Paolisso, M., Secor, D. et al.** (2010).
871 Potential climate change impacts on the Chesapeake Bay. *Estuarine, Coastal and Shelf*
872 *Science* **86**, 1-20.

873 **Pall, P., Aina, T., Stone, D. A., Stott, P. A., Nozawa, T., Hilberts, A. G.,**
874 **Lohmann, D. and Allen, M. R.** (2011). Anthropogenic greenhouse gas contribution to
875 flood risk in England and Wales in autumn 2000. *Nature* **470**, 382-5.

876 **Perdiz, D., Mackeh, R., Pous, C. and Baillet, A.** (2011). The ins and outs of
877 tubulin acetylation: more than just a post-translational modification? *Cellular Signaling*
878 **23**, 763-71.

879 **Pörtner, H. O.** (2010). Oxygen- and capacity-limitation of thermal tolerance: a
880 matrix for integrating climate-related stressor effects in marine ecosystems. *Journal of*
881 *Experimental Biology* **213**, 881-893.

882 **Rawson, P. D., Agrawal, V. and Hilbish, T. J.** (1999). Hybridization between
883 blue mussels *Mytilus galloprovincialis* and *M. trossulus* along the Pacific coast of North
884 America: evidence for limited introgression. *Marine Biology* **134**, 201-211.

885 **Salway, J. G.** (2004). *Metabolism at a Glance*. Oxford: Blackwell Publishing Ltd.

886 **Schneider, K. R.** (2008). Heat stress in the intertidal: comparing survival and
887 growth of an invasive and native mussel under a variety of thermal conditions. *Biological*
888 *Bulletin* **215**, 253-264.

889 **Schneider, K. R. and Helmuth, B.** (2007). Spatial variability in habitat
890 temperature may drive patterns of selection between an invasive and native mussel

891 species. *Marine Ecology Progress Series* **339**, 157-167.

892 **Seed, R.** (1992). Systematics, evolution and distribution of mussels belonging to
893 the genus *Mytilus*: an overview. *American Malacological Bulletin* **117**, 123-137.

894 **Serafini, L., Hann, J. B., Kültz, D. and Tomanek, L.** (2011). The proteomic
895 response of sea squirts (genus *Ciona*) to acute heat stress: A global perspective on the
896 thermal stability of proteins. *Comparative Biochemistry and Physiology, Part D* **6**, 322-
897 334.

898 **Silacci, P., Mazzolai, L., Gauci, C., Stergiopulos, N., Yin, H. L. and Hayoz, D.**
899 (2004). Gelsolin superfamily proteins: key regulators of cellular functions. *Cellular and*
900 *Molecular Life Sciences* **61**, 2614-2623.

901 **Silverman, M. A. and Leroux, M. R.** (2009). Intraflagellar transport and the
902 generation of dynamic, structurally and functionally diverse cilia. *Trends in Cell Biology*
903 **19**, 306-316.

904 **Sternlicht, H., Farr, G. W., Sternlicht, M. L., Driscoll, J. K., Willison, K. and**
905 **Yaffe, M. B.** (1993). The T-complex polypeptide 1 complex is a chaperonin for tubulin
906 and actin *in vivo*. *Proceedings of the National Academy of Sciences of the United States*
907 *of America* **90**, 9422-9426.

908 **Storch, J. and Thumser, A. E.** (2000). The fatty acid transport function of fatty
909 acid-binding proteins. *Biochimica et Biophysica Acta* **1486**, 28-44.

910 **Sugano, Y.** (2009). DyP-type peroxidases comprise a novel heme peroxidase
911 family. *Cellular and Molecular Life Sciences* **66**, 1387-1403.

912 **Thelin, W. R., Hodson, C. A. and Milgram, S. L.** (2005). Beyond the brush
913 border: NHERF4 blazes new NHERF turf. *Journal of Physiology* **567**, 13-19.

914 **Tomanek, L.** (2008). The importance of physiological limits in determining
915 biogeographical range shifts due to global climate change: The heat-shock response
916 *Physiological and Biochemical Zoology* **81**, 709-717.

917 **Tomanek, L.** (2010). Variation in the heat shock response and its implication for
918 predicting the effect of global climate change on species' biogeographic distribution
919 ranges and metabolic costs. *The Journal of Experimental Biology* **213**, 971-979.

920 **Tomanek, L.** (2011). Environmental proteomics: Changes in the proteome of
921 marine organisms in response to environmental stress, pollutants, infection, symbiosis

922 and development. *Annual Review of Marine Sciences* **3**, 373-399.

923 **Tomanek, L.** (2012). Environmental proteomics of the mussel *Mytilus*:
924 implications for stress tolerance and biogeographic range limits in response to climate
925 change. *Integrative and Comparative Biology*, in press.

926 **Tomanek, L. and Zuzow, M. J.** (2010). The proteomic response of the mussel
927 congeners *Mytilus galloprovincialis* and *M. trossulus* to acute heat stress: implications
928 for thermal tolerance and metabolic costs of thermal stress. *Journal of Experimental*
929 *Biology* **213**, 3559-3574.

930 **Tomanek, L., Zuzow, M. J., Ivanina, A. V., Beniash, E. and Sokolova, I. M.**
931 (2011). Proteomic response to elevated P_{CO2} level in eastern oyster, *Crassostrea*
932 *virginica*: evidence for oxidative stress. *Journal of Experimental Biology* **214**, 1836-
933 1844.

934 **Vaidya, V. S., Ferguson, M. A. and Bonventre, J. V.** (2008). Biomarkers of
935 acute kidney injury. *Annual Review of Pharmacology and Toxicology* **48**, 463-493.

936 **van der Wijk, T., Tomassen, S. F., Houtsmuller, A. B., de Jonge, H. R. and**
937 **Tilly, B. C.** (2003). Increased vesicle recycling in response to osmotic cell swelling.
938 Cause and consequence of hypotonicity-provoked ATP release. *Journal of Biological*
939 *Chemistry* **278**, 40020-40025.

940 **Wong, E. and Cuervo, A. M.** (2012). Integration of clearance mechanisms: the
941 proteasome and autophagy. In *Protein Homeostasis*, eds. R. I. Morimoto D. J. Selkoe
942 and J. W. Kelley), pp. 47-65. New York: Cold Spring Harbor Press.

943 **Zhao, S., Xu, W., Jiang, W., Yu, W., Lin, Y., Zhang, T., Yao, J., Zhou, L.,**
944 **Zeng, Y., Li, H. et al.** (2010). Regulation of cellular metabolism by protein lysine
945 acetylation. *Science* **327**, 1000-1004.

946

947

948

949 **Figure legends:**

950

951 **Figure 1:** Proteome maps generated from all 2D gel images of *Mytilus trossulus* (A) and
952 *M. galloprovincialis* (B) gill tissue after exposure of whole animals to a 4 h hyposaline
953 stress (24.5 and 29.8 psu) and a control (35.0 psu) followed by a 0 and 24 h recovery (at
954 ambient 35.0 psu), and through separation of proteins by isoelectric point (horizontal
955 axis) and mass (vertical axis). Each map represents a composite gel image of all thirty-
956 one and thirty-six gels (N=4-6 per treatment; 6 treatments per species), depicting 336 and
957 310 protein spots from gill tissue of *M. trossulus* and *M. galloprovincialis*, respectively.
958 The proteome maps represent average pixel volumes for each protein spot. Numbered
959 spots were those that showed changes in abundance in response to hyposaline stress (two-
960 way ANOVA with permutations, $p < 0.02$) and were identified using tandem mass
961 spectrometry (for protein identifications see supplemental material, including Tables S1
962 and S2).

963

964 **Figure 2:** Principal component analyses of hyposaline treatments for (A) *M. trossulus*
965 and (B) *M. galloprovincialis*, using proteins that were significant for a main salinity
966 effect (two-way ANOVA with permutations). Each symbol represents a mussel treated
967 to a different salinity (for 4 h) without (0 h) and with a 24 h recovery at 35.0 psu. In each
968 panel the horizontal axis represents PC1, and the vertical axis represents PC2.
969 Percentages represent the proportion of total variation in the dataset described by each
970 component. For matching loadings of proteins contributing to PC1 and PC2 see
971 supplemental material.

972

973 **Figure 3:** Principal component analyses of hyposaline treatments for (A) *M. trossulus*
974 and (B) *M. galloprovincialis*, using proteins that were significant for a main time effect
975 during recovery (two-way ANOVA with permutations). For further details see Fig. 2.

976

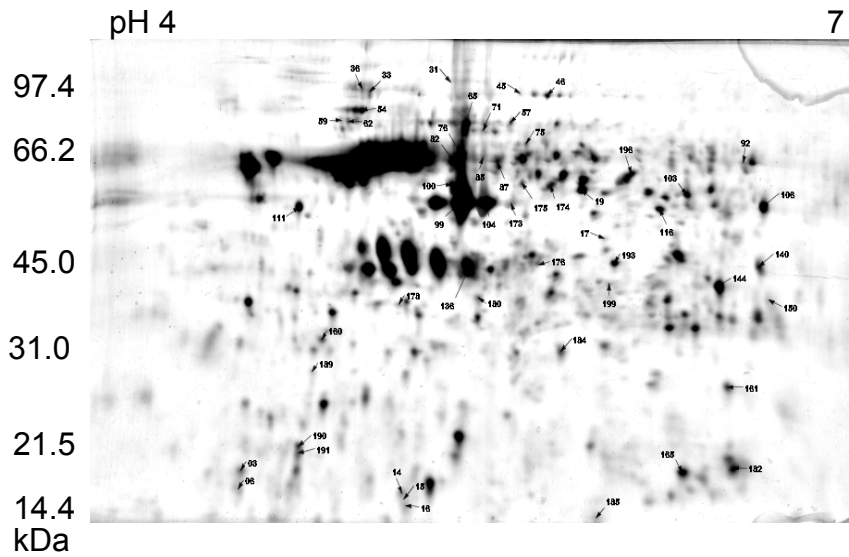
977 **Figure 4:** Hierarchal clustering using Pearson's correlation of proteins involved in
978 protein chaperoning and degradation from (A) *Mytilus trossulus* and (B) *M.*
979 *galloprovincialis* that changed significantly with hyposaline stress and were identified
980 with tandem mass spectrometry. Blue coloring represents a lower than average protein
981 abundance (standardized volume), whereas orange represents greater than average protein
982 abundance. The columns show individual mussels, which cluster according to treatment
983 ($N= 4-6$ for each treatment for *M. trossulus* and $N=6$ for *M. galloprovincialis*). The rows
984 represent the standardized protein abundances, which are identified to the right. Clusters
985 talked about in the text are labeled for species (T versus G), general functional category
986 (CH= chaperoning, E=energy metabolism, and C=cytoskeleton), and cluster (starting
987 with A). Clusters do not adhere to specific criteria other than that they show similar
988 changes in protein abundance that are considered in the text. Statistical significance is
989 given for each of the two main effects (S=salinity and T=time) and the interaction effect
990 (I=interaction) in the column to the right of the protein identification.

991

992 **Figure 5:** Hierarchal clustering using Pearson's correlation of proteins involved in energy
993 metabolism and oxidative stress from (A) *Mytilus trossulus* and (B) *M. galloprovincialis*
994 that changed significantly with hyposaline stress. For further details see Fig. 4.

995 **Figure 6:** Hierarchical clustering using Pearson's correlation of proteins involved in
996 cytoskeleton, actin regulation and vesicle transport from (A) *Mytilus trossulus* and (B) *M.*
997 *galloprovincialis* that changed significantly with hyposaline stress. For further details see
998 Fig. 4.
999
1000
1001

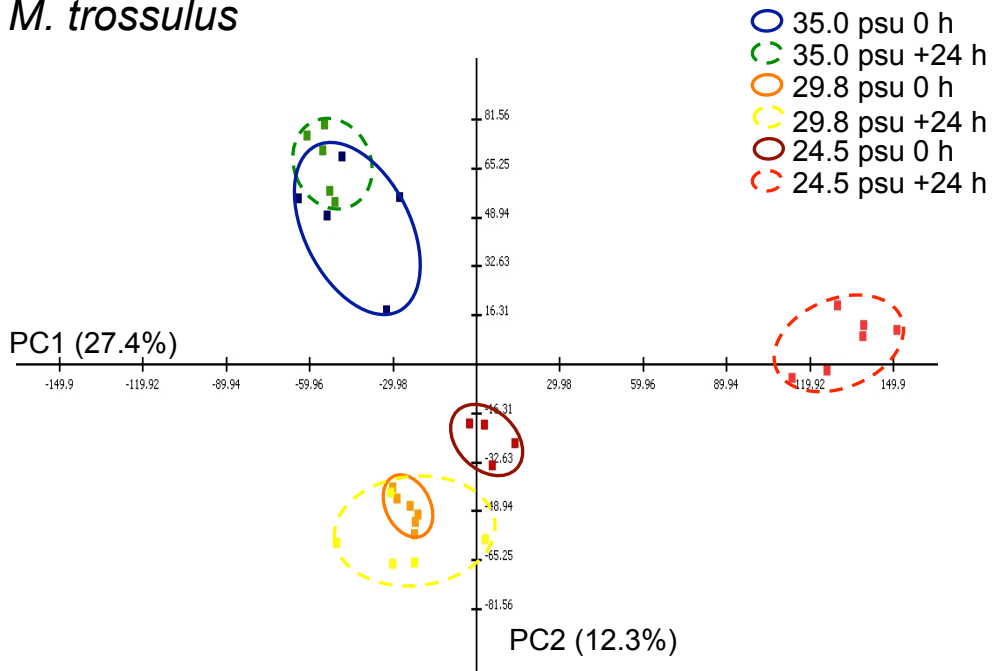
(A) *M. trossulus*



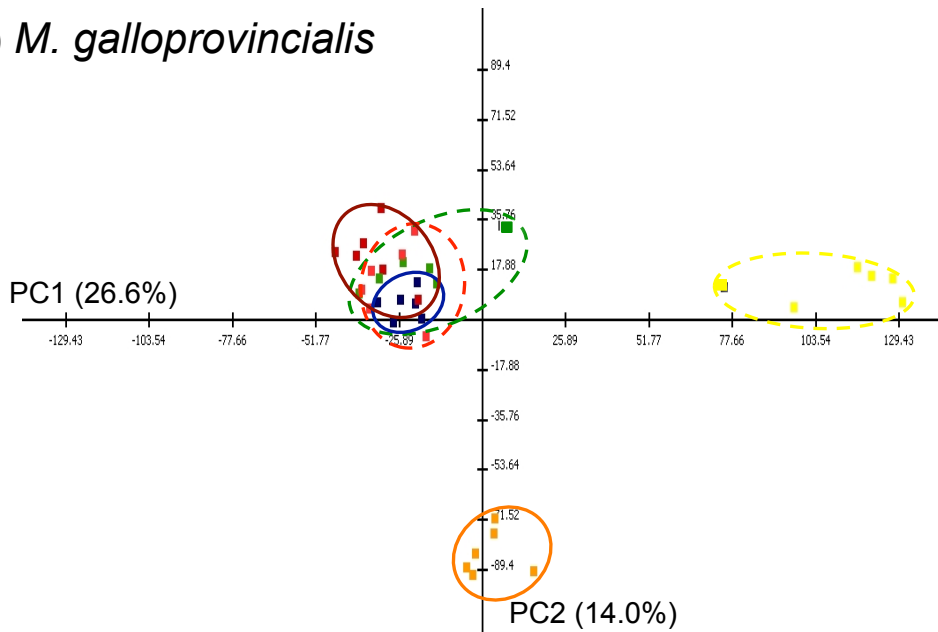
(B) *M. galloprovincialis*



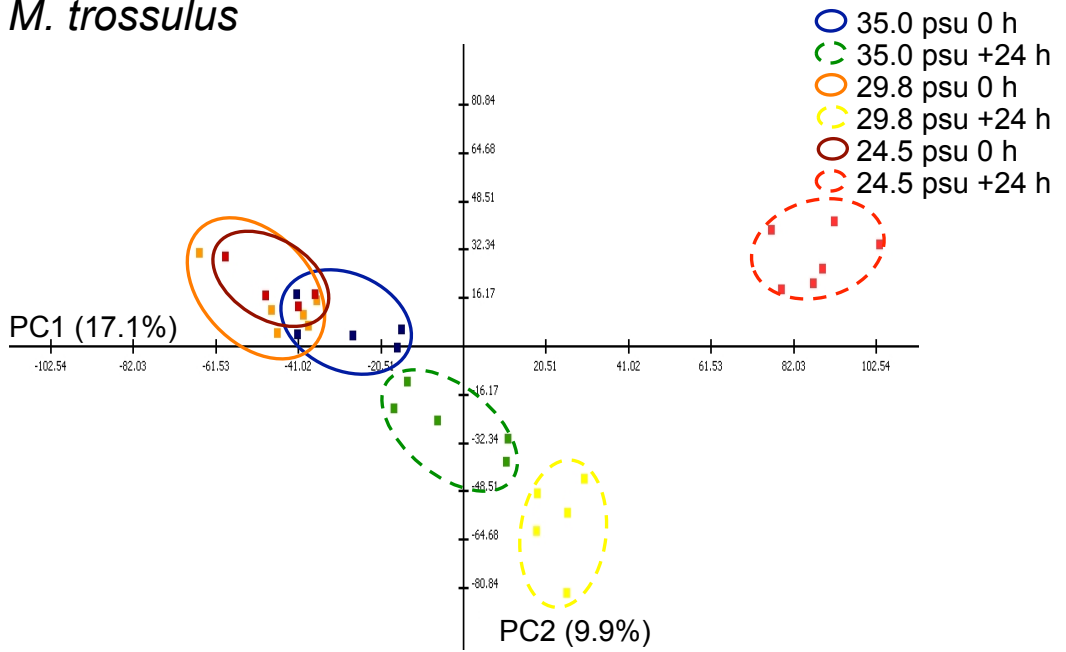
(A) *M. trossulus*



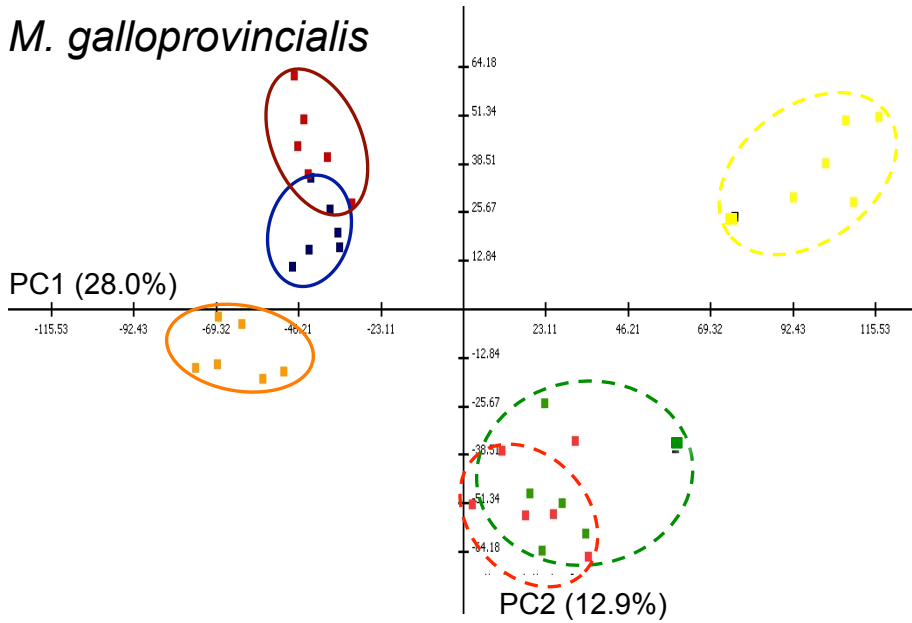
(B) *M. galloprovincialis*

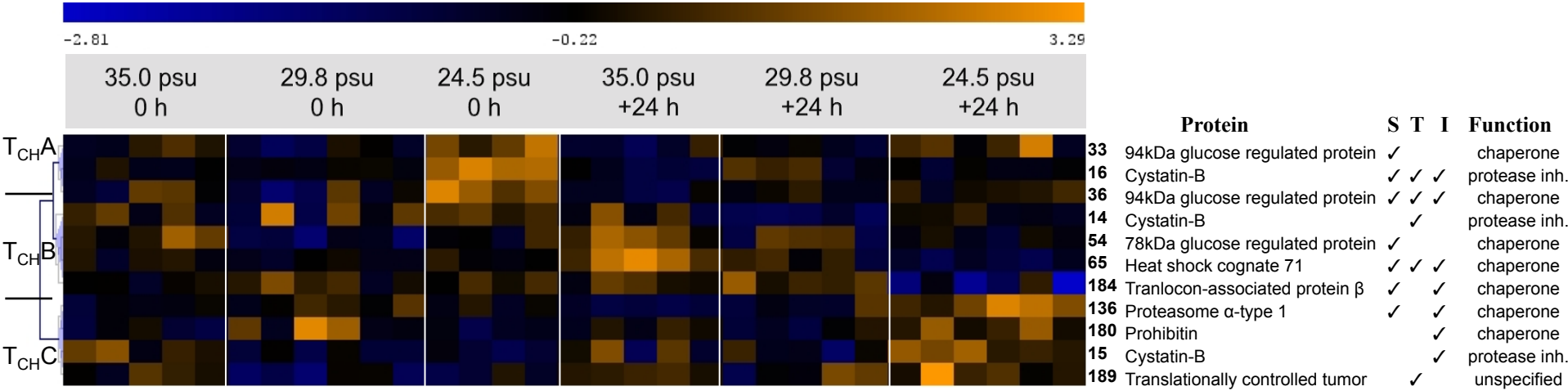
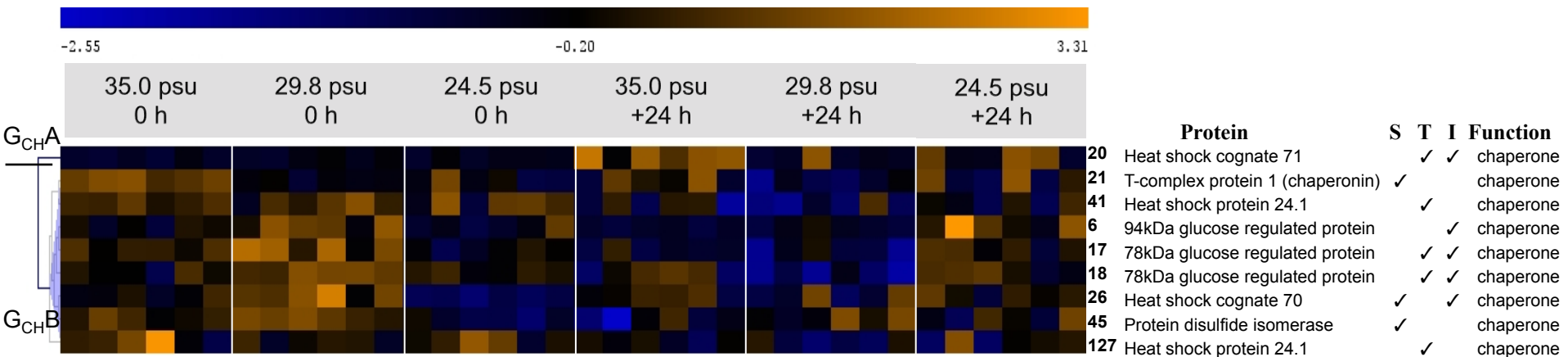


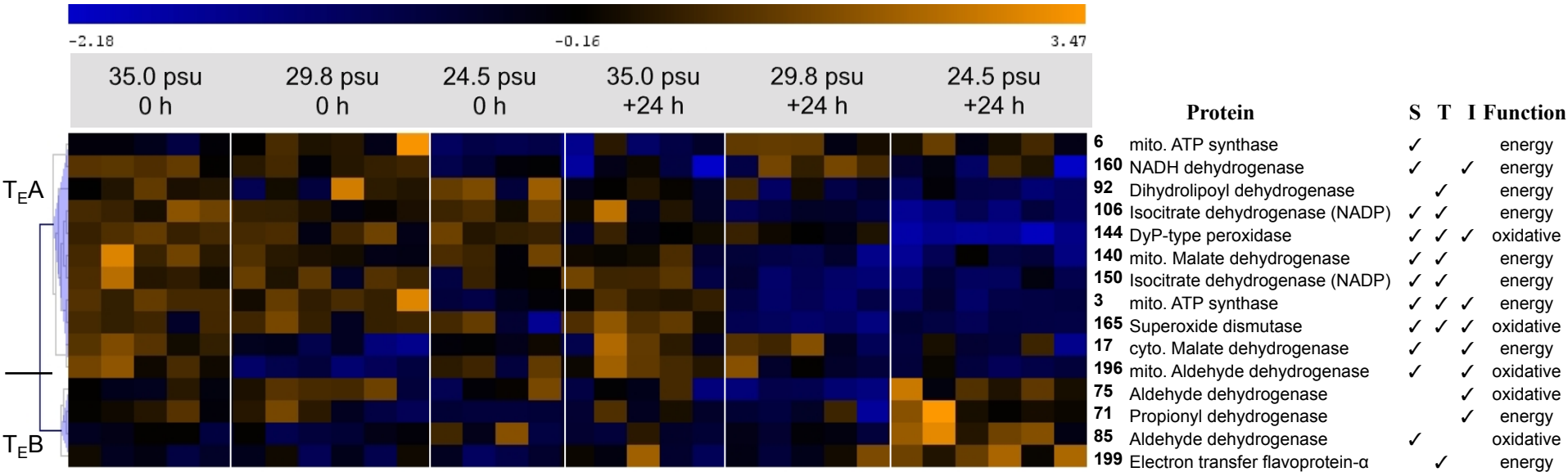
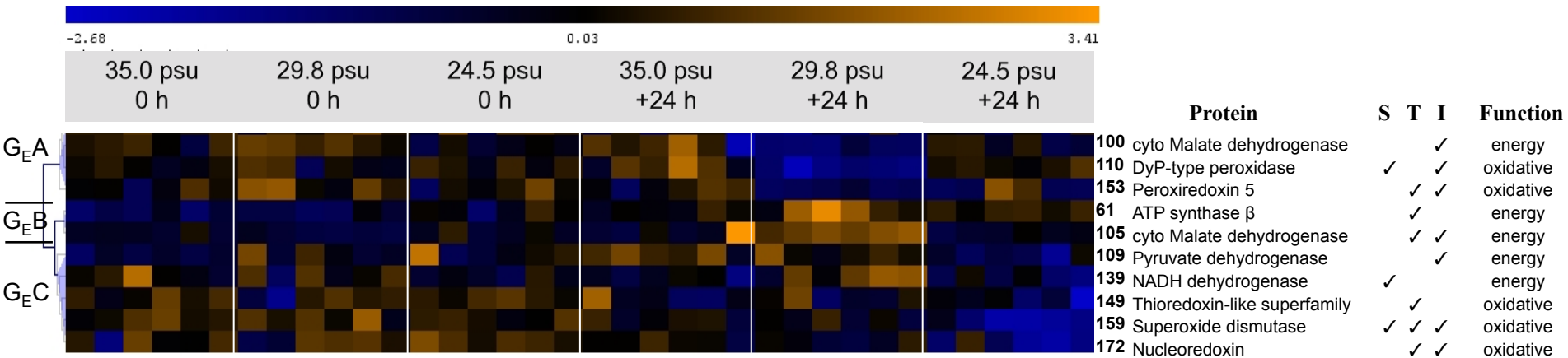
(A) *M. trossulus*



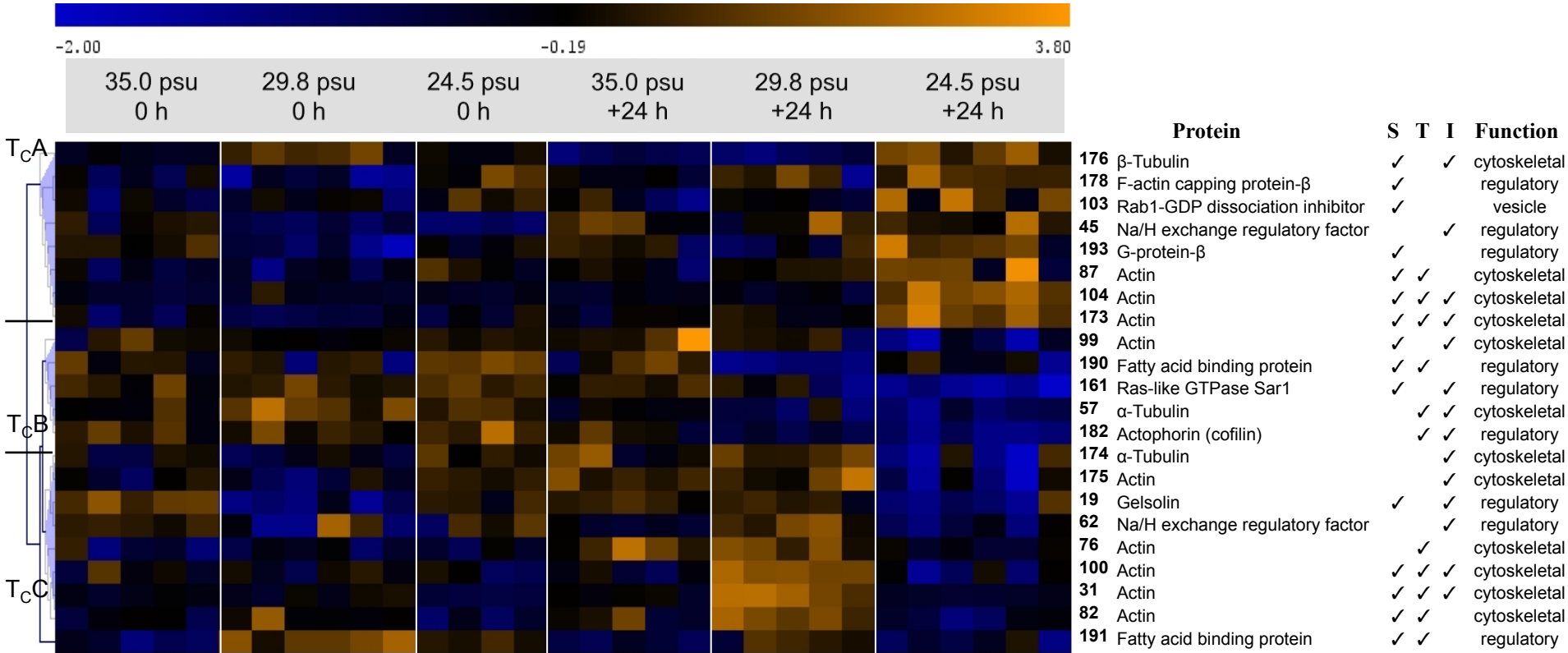
(B) *M. galloprovincialis*



(A) *M. trossulus*- Molecular chaperones, protein degradation and protease inhibition(B) *M. galloprovincialis* – Molecular chaperones

(A) *M. trossulus*- Energy metabolism and oxidative stress proteins(B) *M. galloprovincialis*- Energy metabolism and oxidative stress proteins

(A) *M. trossulus* - Actin regulation, cytoskeletal elements and vesicle transport



(B) *M. galloprovincialis*- Actin regulation, cytoskeletal elements and vesicle transport